Origin of the "Waterfall" Effect in Phonon Dispersion of Relaxor Perovskites

J. Hlinka, S. Kamba, and J. Petzelt

Institute of Physics, Academy of Sciences of the Czech Republic, Na Slovance 2, 18221 Praha 8, Czech Republic

J. Kulda

Institute Laue-Langevin, Avenue des Martyrs, 38640 Grenoble, France

C. A. Randall and S. J. Zhang

Materials Research Institute, Pennsylvania State University, University Park, Pennsylvania 16802, USA

We have undertaken an inelastic neutron scattering study of the perovskite relaxor ferroelectric $Pb(Zn_{1/3}Nb_{2/3})O_3$ with 8% $PbTiO_3$ (PZN-8%PT) in order to elucidate the origin of the previously reported unusual kink on the low frequency transverse phonon dispersion curve (known as the "waterfall effect"). We show that its position (q_{wf}) depends on the choice of the Brillouin zone and that the relation of q_{wf} to the size of the polar nanoregions is highly improbable. The waterfall phenomenon is explained in the framework of a simple model of coupled damped harmonic oscillators representing the acoustic and optic phonon branches.

Ferroelectric perovskites $Pb(Zn_{1/3}Nb_{2/3})O_3$ (PZN) and $Pb(Mg_{1/3}Nb_{2/3})O_3$ (PMN) and related materials have recently attracted a great deal of attention, among others, due to the excellent piezoelectric properties [1] of their solid solutions with $PbTiO_3$. Their average ABO_3 perovskite structure is perturbed by a short-range occupational ordering on *B*-site positions [2,3]. It is known that this nanoscopic inhomogeneity is responsible for relaxor properties of these materials, such as smearing and frequency dependence of the dielectric anomaly associated with the ferroelectric ordering [4], and for other phenomena reflecting the presence of polar nanoregions (PNR) persisting hundreds of Kelvins above the temperature of the dielectric permittivity maximum [5]. Unfortunately, it is not easy to deal with these inhomogeneities in a simple enough model, and the understanding of the relaxor properties is not yet satisfactory.

Since these materials are available as large single crystals, inelastic neutron scattering can be used to study the phonon dispersion curves. The spectrum of the lowest frequency transverse excitations usually consists of interacting and mutually repelling transverse acoustic and transverse optic phonon branches. It is known that upon approaching a displacive ferroelectric phase transition, the lowest zone center optic mode (soft mode) tends to zero frequency. Instead of that, it was repeatedly found that near the "smeared" phase transition of relaxor ferroelectrics, the upper branch appears to drop precipitously into the lower branch at a finite value of momentum transfer of the order of $q_{wf} = 0.2$ Å^{-1}. For explanation of this "waterfall effect," Gehring, Park, and Shirane [6] proposed that the characteristic wave vector q_{wf} corresponds to the size of the PNR's, and that due to these

PNR's the soft branch phonons with $q < q_{wf}$ cannot effectively propagate in the crystal. The idea was subsequently specified within a mode-coupling model [7,8] assuming a sharp increase of transverse optic branch damping (inverse lifetime) for $q < q_{wf}$.

Within the past three years, it was established that the waterfall effect is common to a number of relaxor ferroelectrics, including PZN [7,9], PMN [10–12], $Pb(Zn_{1/3}Nb_{2/3})O_3$ with 8% $PbTiO_3$ (PZN-8%PT) [6], PZN-15%PT [13], and PMN-20%PT [14]. However, we have noticed that the sharp drop (near $q \approx 0.2$ Å^{-1}) of the dispersion curves of the single-domain tetragonal $BaTiO_3$ drawn in Fig. 6 of Ref. [15] also strikingly closely resembles those of the relaxors (compare, for example, with Fig. 2 of Ref. [6]). Obviously, the explanation based on the characteristic size of PNR's cannot be valid for an experiment performed on a classic single-domain ferroelectric crystal. This Letter brings new inelastic neutron scattering data showing that such an explanation does not hold for relaxors either. We demonstrate that the waterfall effect can be ascribed to an entirely classic interference of line shape anomalies due to the coupled acoustic and optic branches without any *ad hoc* assumption of an anomalous increase of the bare optic branch damping below q_{wf}.

For the experiment we have chosen a 3.7 g single crystal of PZN-8%PT, used already in our previous neutron study [16]. This as-grown, optically transparent, yellowish single crystal was produced by the high temperature flux technique at the Materials Research Institute, Pennsylvania State University. This promising PZN-8%PT material, showing both relaxor and giant piezoelectric properties, has been studied recently by a

number of techniques, and it is the one for which the possible relation of q_{wf} to the size of PNR's was first invoked [6].

The present experiment was carried out on the recently upgraded IN8 thermal neutron spectrometer at the ILL high flux reactor. The instrument was operated with a fixed wave number of scattered neutrons $k_f = 3\ \text{Å}^{-1}$, using horizontally focusing (vertically flat) Si crystals as monochromator and analyzer. The sample was wrapped in a thin Nb foil and mounted in a vacuum furnace allowing us to reach temperatures up to 1200 K with a stability better than 1 K. The sample was oriented with the cubic [001] axis vertical. This geometry allowed us to explore the $(hk0)$ scattering plane. Both transverse and longitudinal momentum resolution widths measured on the (030) Bragg reflection were better than 0.07 and 0.06 of a reciprocal lattice unit (rlu, where 1 rlu is $2\pi/a \approx 1.55\ \text{Å}^{-1}$), respectively. This is about equivalent to resolution widths in a setup with flat PG (pyrolitic graphite) crystals and 40' Soller collimators used in the previous studies by other authors. The present setup using elastically bent Si crystals [17] permits one to avoid spurious effects from tails of reflection curves inherent to PG mosaic crystals and provides an improved energy resolution of 0.8 meV (FWHM), as given by the energy profile of elastic incoherent scattering from our crystal and confirmed by an independent measurement on a vanadium reference sample.

The typical constant energy transverse scans in the 020 and 030 Brillouin zones at 500 K are displayed in Fig. 1, and the positions of their maxima are plotted as solid symbols in Fig. 2. The apparent dispersion curve obtained in this way from the 020 Brillouin zone data has an almost vertical rise up near $q_{wf} = 0.13$ rlu. This value corresponds exactly to the q_{wf} obtained from the 220 zone data at the same temperature and same crystallographic direction for this material in Ref. [6].

On the other hand, the position of the upward rise observed by us in the 030 Brillouin zone is at a significantly smaller value of $q_{wf} \approx 0.06$ rlu. As the same [010]-polarized modes with wave vectors along [100] are probed in both Brillouin zones, the value of q_{wf} can hardly provide a measure of the size of PNR's [6]. On the contrary, the remarkable dependence of q_{wf} on the chosen Brillouin zone proves that the observed dispersion is merely an apparent dispersion. In fact, it is known that maximum intensity positions for the response function of coupled damped harmonic phonons can be sensitive to the dynamical structure factors (chosen Brillouin zone) [18]. Furthermore, the striking difference between the 030 zone value of q_{wf} and almost the same values of q_{wf} in 020 and 220 zones indicates that the waterfall effect is related to the dynamical structure factor of the bare acoustic branch, which is known to be very small in the 030 zone [11,19].

As a matter of fact, it turns out that the waterfall effect can be reproduced in a quite simple model. Let us con-
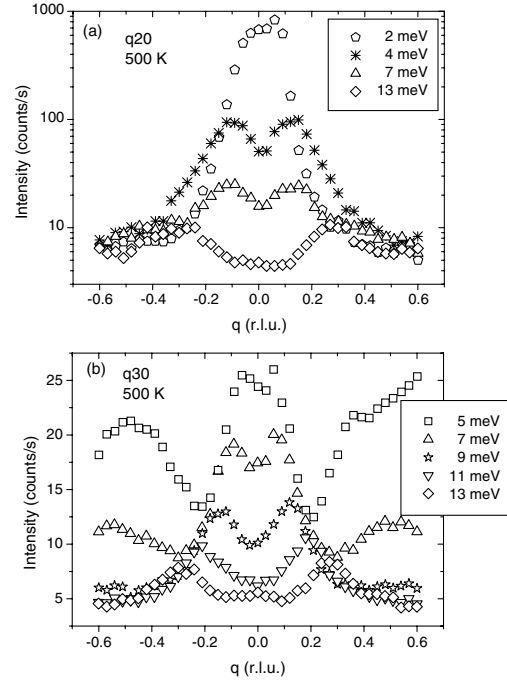

FIG. 1. Low frequency phonon modes in PZN-8%PT measured by constant energy scans at 500 K. Measurements were performed in (a) a 020 Brillouin zone [$Q = (q20)$ scans] and in (b) a 030 Brillouin zone [$Q = (q30)$ scans].

sider the standard model [20–22] of two coupled damped harmonic oscillators, defined by a 2×2 dynamical and damping matrices $\mathbf{D}_q$ and $\mathbf{\Gamma}_q$

$$\mathbf{D}_q = \begin{pmatrix} \omega_{TA}^2(q) & \Delta(q) \\ \Delta(q)^* & \omega_{TO}^2(q) \end{pmatrix}, \qquad (1)$$

$$\mathbf{\Gamma}_q = \begin{pmatrix} \Gamma_{TA}(q) & \Gamma_{AO}(q) \\ \Gamma_{AO}(q) & \Gamma_{TO}(q) \end{pmatrix}, \qquad (2)$$
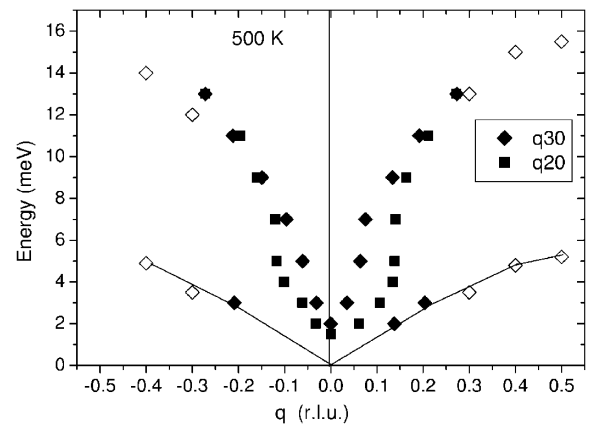

FIG. 2. Position of maxima in constant energy transverse scans performed in 0 2 0 (solid squares) and 0 3 0 (solid diamonds) Brillouin zones (as in Fig. 1). Maxima are forming two distinct "dispersion curves." The inflection points near $q_{wf} = 0.13$ and 0.06 rlu, respectively, are discussed in the text. Open symbols show maximum intensity positions in constant-q scans. Lines are only guides for the eye.

where $\omega_{TA}(q)$ and $\omega_{TO}(q)$ describe dispersions of bare acoustic and optic branches, $\Delta(q)$ describes their mutual bilinear interaction, $\Gamma_{TA}(q)$ and $\Gamma_{TO}(q)$ stand for bare mode frequency independent damping, $\Gamma_{AO}(q)$ stands for viscous interaction (bilinear in time derivatives of bare mode coordinates) and q is the reduced phonon wave vector in a chosen direction (in this Letter, along the cubic [100]). In the high temperature limit ($h\omega \ll kT$), the corresponding inelastic neutron scattering intensity is proportional to [18,21]

$$I(\omega, q) = kT\omega^{-1}\mathbf{f}(q)^*\text{Im}[\mathbf{G}(\omega, q)]\mathbf{f}(q), \qquad (3)$$

$$\mathbf{G}(\omega, q) = (\mathbf{D}_q - i\omega\mathbf{\Gamma}_q - \omega^2\mathbf{E})^{-1}, \qquad (4)$$

where $\mathbf{E}$ is a 2×2 unit matrix and $f(q)$ is a 2-component vector composed of dynamical structure factors of bare acoustic and optic branches, respectively. At small frequencies, it is expected that $\omega|\Gamma_{AO}(q)| \ll |\Delta_q|$ so that, as, e.g., in Ref. [18], $\Gamma_{AO}(q) = 0$ will be assumed in the following. The wave vector dependence of dynamical matrix $\mathbf{D}_q$ can be conveniently cast in the form which appears in the simplest nearest-neighbor interaction models with 2 degrees of freedom per unit cell [23–25]:

$$\omega_{TA}^2(q) = A\sin^2(\pi q/2), \qquad (5)$$

$$\omega_{TO}^2(q) = c + B\sin^2(\pi q/2), \qquad (6)$$

$$\Delta_q = d\sin^2(\pi q/2), \qquad (7)$$

where the real parameters A, B, c, and d define the strength of dispersion of bare acoustic and optic branches, the square of soft mode frequency, and the strength of mode mixing at the zone boundary, respectively. Let us note that the dynamical matrix parametrized in this way shows the same asymptotic behavior for $q \to 0$ as the standard model of Ref. [26], and at the same time provides the correct dispersion behavior also at the zone boundary. In the same spirit, we introduce

$$\Gamma_{TA}(q) = g\sin^2(\pi q/2), \qquad (8)$$

$$\Gamma_{TO}(q) = h, \qquad (9)$$

where the real parameters g and h define the damping of the bare acoustic branch (with required asymptotic q^2 dependence) and the q-independent damping of the bare optic mode, respectively.

Numerical calculations were performed for a set of realistic values ($A = 100$ meV^2, $B = 150$ meV^2, $c = 15$ meV^2, $d = 100$ meV^2, $g = 6$ meV, and $h = 6$ meV). Constant energy profiles calculated for the case of equal bare acoustic and optic structure factors ($\mathbf{f} = (0.5, 0.5)$) are shown in Fig. 3, while phonon dispersion curves obtained by diagonalization of the dynamical matrix $\mathbf{D}_q$ are shown in Fig. 4. Figure 4 also shows that the positions of the maximum intensity in constant energy
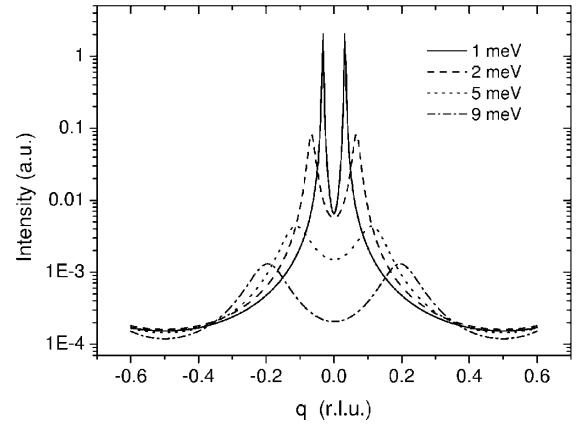
FIG. 3. Constant energy scans at 1–9 meV simulated from the model described in the text, for structure factors $\mathbf{f} = (0.5, 0.5)$.

profiles shown in Fig. 3 form an apparent dispersion branch which follows the acoustic branch for small q, but then it sharply rises towards the upper phonon branch near 0.1 rlu. The shape of this apparent dispersion curve indeed corresponds well with the experimental findings shown, for example, in Fig. 2.

As expected, the waterfall region of the apparent dispersion curve depends noticeably on the dynamical structure factor. For example, a decrease of the weight of the bare acoustic structure factor shifts the waterfall position towards the zone center, as it follows from Fig. 4. A similar tendency is found in the experimental data taken in the "predominantly optic" 030 Brillouin zone (Fig. 2). In the limit of the zero bare acoustic structure factor [$\mathbf{f} = (0, 1)$], the waterfall wave vector is zero (Fig. 5). On the
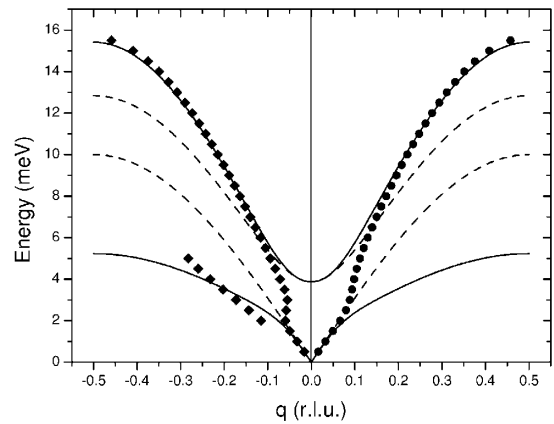
FIG. 4. Dispersion curves calculated from the model described in the text. Full and dashed lines correspond to frequencies of repelled and bare phonon branches obtained as square roots of eigenvalues and of diagonal elements of the dynamical matrix $\mathbf{D}_q$, respectively. Full circles (on the right side) stand for positions of maximum intensity in constant energy profiles shown in Fig. 3, calculated for balanced structure factors $\mathbf{f} = (0.5, 0.5)$. Full diamonds (left side of diagram) are calculated in the same way for the case of a smaller bare acoustic structure factor [$\mathbf{f} = (0.25, 0.75)$].
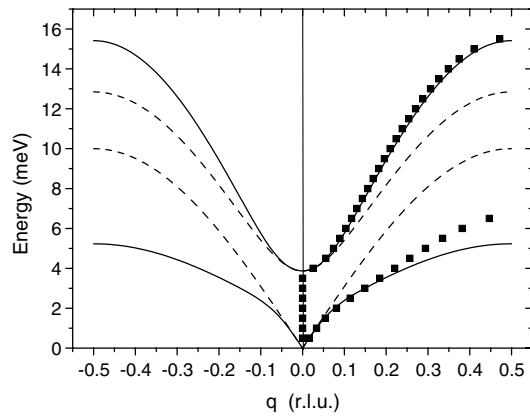
FIG. 5.   Dispersion curves calculated from the model described in the text. Symbols have the same meaning as in Fig. 4; full squares are calculated from constant energy profiles calculated for the case of the zero bare acoustic structure factor $[\mathbf{f} = (0, 1)]$.

other hand, with a slight change of parameters, the apparent waterfall dispersion curve can attain even a negative slope. These results show that the constant energy scan technique for the investigation of coupled acoustic-optic branches should be used with certain caution. More detailed discussion of the model properties and quantitative analysis of the experimental data is beyond the scope of this Letter and will be published elsewhere.

In conclusion, we argue that the waterfall kink seen on the dispersion curves of several relaxor perovskites can be explained in the framework of coupled damped harmonic oscillator models describing the interaction of the acoustic and optic branches. This kink appears only on an apparent dispersion curve, obtained from the maxima of constant energy sections of scattered intensity, while no such kink is present in the dispersion of bare or coupled branches themselves. In the light of these results, there is no reason for the position q_{wf} of the waterfall kink to be related to the size of the polar nanoregions. First of all, there is no need to assume the unusual increase of bare optic branch damping below the waterfall wave vector q_{wf} in the present model. Secondly, the waterfall position is very sensitive to the dynamical structure factor both in our model and in our experimental data, where it becomes reduced by as much as a factor of 2 when passing from the 020 to 030 Brillouin zone. It also follows that the waterfall anomaly in the low-energy phonon dispersion is not specific to relaxor ferroelectrics, but it can be encountered in other systems with interacting acoustic and soft optic branches, such as the ferroelectric perovskite $BaTiO_3$.

[1] S. E. Park and T. R. Shrout, J. Appl. Phys. **82**, 1804 (1997).
[2] A. D. Hilton, D. J. Barber, C. A. Randall, and T. R. Shrout, J. Mater. Sci. **25**, 3461 (1990).
[3] C. A. Randall and A. S. Bhala, Jpn. J. Appl. Phys. **29**, 327 (1990).
[4] N. Setter and L. E. Cross, J. Appl. Phys. **51**, 4356 (1980); F. Chu, N. Setter, and A. K. Tagantsev, J. Appl. Phys. **74**, 5129 (1993).
[5] G. Burns and F. H. Dacol, Ferroelectrics **52**, 103 (1983); Solid State Commun. **48**, 853 (1983).
[6] P. M. Gehring, S. E. Park, and G. Shirane, Phys. Rev. Lett. **84**, 5216 (2000).
[7] P. M. Gehring, S. E. Park, and G. Shirane, Phys. Rev. B **63**, 224109 (2001).
[8] G. Shirane and P. M. Gehring, J. Phys. Soc. Jpn. **70**, 227 (2001).
[9] I. Tomeno, S. Shimanuki, Y. Tsunoda, and Y. Y. Ishii, J. Phys. Soc. Jpn. **70**, 1444 (2001).
[10] P. M. Gehring, S. B. Vakhrushev, and G. Shirane, in *Fundamental Physics of Ferroelectrics 2000: Aspen Center for Physics Winter Workshop*, edited by R. E. Cohen, AIP Conf. Proc. No. 535 (AIP, New York, 2000), p. 314.
[11] S. Wakimoto, C. Stock, Z.-G. Ye, W. Chen, P. M. Gehring, and G. Shirane, Phys. Rev. B **66**, 224102 (2002).
[12] P. M. Gehring, S. Wakimoto, Z.-G. Ye, and G. Shirane, Phys. Rev. Lett. **87**, 277601 (2001).
[13] D. La-Orauttapong, B. Noheda, Z.-G. Ye, P. M. Gehring, J. Toulouse, D. E. Cox, and G. Shirane, Phys. Rev. B **65**, 144101 (2002).
[14] T. Y. Koo, P. M. Gehring, G. Shirane, V. Kiryukhin, S. G. Lee, and S. W. Cheong, Phys. Rev. B **65**, 144113 (2002).
[15] G. Shirane, J. D. Axe, and J. Harada, and A. Linz, Phys. Rev. B **2**, 3651 (1970).
[16] J. Hlinka, S. Kamba, J. Petzelt, J. Kulda, C. A. Randall, and S. J. Zhang, J. Phys. Condens. Matter **15**, 4249 (2003).
[17] J. Kulda and J. Šaroun, Nucl. Instrum. Methods Phys. Res., Sect. A **379**, 155 (1996).
[18] J. Harada, J. D. Axe, and G. Shirane, Phys. Rev. B **4**, 155 (1971).
[19] S. B. Vakhrushev and S. M. Shapiro, Phys. Rev. B **66**, 214101 (2002).
[20] A. S. Barker and J. J. Hopfield, Phys. Rev. **135**, A1732 (1964).
[21] R. Currat, H. Buhay, C. H. Perry, and A. M. Quittet, Phys. Rev. B **40**, 10 741 (1989).
[22] J. Hlinka, I. Gregora, and V. Vorlíček, Phys. Rev. B **56**, 13 855 (1997).
[23] I. Etxebarria, M. Quilichini, J. M. Perez-Mato, P. Boutrouille, F. J. Zuniga, and T. Breczewski, J. Phys. Condens. Matter **4**, 8551 (1992).
[24] J. Hlinka, M. Quilichini, R. Currat, and J. F. Legrand, J. Phys. Condens. Matter **8**, 8221 (1996).
[25] Z. Y. Chen and M. B. Walker, Phys. Rev. B **43**, 5634 (1991).
[26] J. D. Axe, J. Harada, and G. Shirane, Phys. Rev. B **1**, 1227 (1969).